Quantum Monte Carlo Calculations of H_2 Dissociation on Si(001)

Claudia Filippi,[1] Sorcha B. Healy,[2] P. Kratzer,[3] E. Pehlke,[4] and M. Scheffler[3]

[1]*Instituut Lorentz, Universiteit Leiden, Niels Bohrweg 2, Leiden, NL-2333 CA, The Netherlands*
[2]*Physics Department, National University of Ireland, Cork, Ireland*
[3]*Fritz-Haber-Institut der Max-Planck-Gesellschaft, Faradayweg 4-6, D-14195 Berlin-Dahlem, Germany*
[4]*Institut für Laser und Plasmaphysik, Universität Essen, 45117 Essen, Germany*

(Received 19 April 2002; published 30 September 2002)

The dissociative adsorption of H_2 on the Si(001) surface is theoretically investigated for several reaction pathways using quantum Monte Carlo methods. Our reaction energies and barriers are at large variance with those obtained with commonly used approximate exchange-correlation density functionals. Our results for adsorption support recent experimental findings, while, for desorption, the calculations give barriers in excess of the presently accepted experimental value, pinpointing the role of coverage effects and desorption from steps.

DOI: 10.1103/PhysRevLett.89.166102 PACS numbers: 68.43.Bc, 68.43.Fg

The dissociative adsorption of molecular hydrogen on the Si(001) surface has become a paradigm in the study of adsorption systems. Despite its apparent simplicity, more than a decade of extensive experimental and theoretical investigations have not clarified fundamental aspects of the chemical reaction of H_2 with this surface. More generally, this failure challenges the theoretical understanding of surface chemical reactions that has evolved from density-functional calculations during the past years.

Many of the experimental observations are hard to reconcile in a unified picture: the sticking probability for dissociative adsorption of H_2 on the clean surface is very small at room temperature, suggesting a high adsorption barrier; sticking increases dramatically with higher surface temperatures [1]. On the other hand, the nearly thermally distributed kinetic energy of desorbing molecules has lead researchers to the conclusion that the molecules have transversed almost no adsorption barrier [2]. Microscopically, these observations were originally interpreted in terms of an intradimer mechanism, where the hydrogen molecule interacts with one single dimer of the Si(001) surface [3]. However, very recent experiments have pointed to additional mechanisms involving not just a single dimer but nearby dimers [4,5]. The existence of highly reactive pathways was first demonstrated on steps [6] or H-precovered surfaces [7], and evidence that H_2 reacts with two adjacent dimers has also now been given for the clean surface [8]. In Fig. 1, the intradimer (H2*) and two interdimer pathways at different coverages (H2 and H4) are schematically shown.

Theoretically, density-functional theory (DFT) calculations performed on intradimer and interdimer mechanisms have lead to limited agreement with experiments. While correctly predicting the existence of a barrierless H4 interdimer reaction path at high coverages [9], previous DFT slab calculations yielded an adsorption barrier for the low-coverage H2* and H2 pathways too low to explain the small sticking coefficient observed at low temperatures [7]. Desorption barriers from DFT obtained within the generalized gradient approximation (GGA) were also generally lower than the experimental value (2.5 eV, Ref. [10]). Additional evidence for a possible inadequacy of DFT-GGA to describe this reaction comes from comparison with highly correlated quantum chemistry calculations for small cluster models of the surface: For the intradimer pathway, these methods obtain values for the desorption barrier that are at large variance with the DFT-GGA value [11–13].

In this Letter, we present a novel combination of techniques to study surface chemical reactions: Quantum Monte Carlo (QMC) methods on large cluster models of the surface are used to improve over DFT slab calculations of reaction energies and energy barriers. QMC has been proven to provide an accurate description of electronic correlation and, over other theoretical approaches, offers the advantage that reliable reaction energetics can be computed for relatively large systems [14]. Our many-body calculations predict reaction energies and barriers noticeably higher than those obtained in DFT, pointing to the inadequacy of the local density approximation or commonly used GGAs to describe the Si-H bond. In

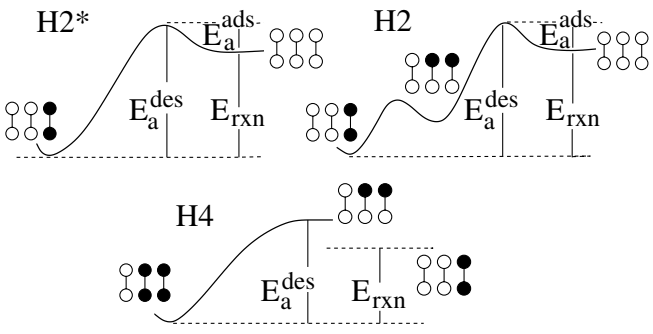

FIG. 1. Intradimer (H2*) and interdimer mechanisms at low (H2) and high (H4) coverages. The surface configuration along the pathway is schematically shown: A circle represents a Si atom and a filled circle H-Si. E_a^{ads}, E_a^{des}, and E_{rxn} are the adsorption, desorption, and reaction energies, respectively.

improvement over previous DFT calculations, the QMC adsorption barriers for the intradimer (H2*) and the low-coverage interdimer (H2) pathways give a theoretical account for the tiny sticking coefficient of H_2 on the clean Si(001) surface. Our results also corroborate the existence of the barrierless high-coverage interdimer (H4) mechanism recently proposed experimentally.

Computational methods.—We employ slabs as well as clusters to mimic the Si(001) surface. The surface can be appropriately modeled with clusters containing only a single row of dimers [15]: interactions are negligible between neighboring dimer rows, while substantial between dimers in the same row. Such clusters with one, two, three, and four dimers are Si_9H_{12}, $Si_{15}H_{16}$, $Si_{21}H_{20}$, and $Si_{27}H_{24}$. They represent a four layer cut of the Si(001) surface with all but the surface atoms terminated with hydrogens to passivate dangling bonds.

As a starting point, plane-wave pseudopotential calculations within DFT were performed to obtain geometries and total energies of both the cluster and slab models. For details on the construction and the geometry of the clusters, see Ref. [16]. We optimized all geometries using the PW91 functional [17], which gives a good description of the structural properties of Si (lattice constant error $<1\%$). Moreover, for cluster models of H_2/Si(001), the geometries optimized using PW91 and the hybrid functional B3LYP [18] were found to be very similar [19], and the energetics of the reaction on both sets of geometries essentially the same within B3LYP (as shown below, B3LYP gives energies very close to our accurate QMC results). It is therefore a sound procedure to use QMC on geometries obtained from PW91 calculations to assess whether a more accurate treatment of electronic correlation can change the physical picture.

The QMC results presented here are from diffusion Monte Carlo (DMC) calculations [20]: DMC is a stochastic method to solve the many-body Schrödinger equation within the fixed-node approximation (i.e., the lowest-energy state with the same nodes as a given trial wave function). The many-body trial wave function is of the Slater-Jastrow form given in Ref. [21] (modified to deal with pseudoatoms). The determinantal part of the wave function is generated within Hartree-Fock or multiconfiguration self-consistent-field method [22], using the quantum chemistry package GAMESS [23]. The parameters in the Jastrow correlation factor are optimized within QMC using the variance minimization method [24].

We calculate the energetics for the intradimer and interdimer pathways of H_2 dissociation on the Si(001) surface using B3LYP and QMC for the cluster geometries and PW91 for both clusters and slab.

Intradimer mechanism.—In the H2* pathway, the hydrogen molecule dissociatively adsorbs on the same Si dimer through an asymmetric transition state (TS). Multireference configuration interaction (MRCI) calculations [13] on Si_9H_{12} yield adsorption and desorption barriers which are 0.3 and 0.8 eV higher than the corresponding PW91 values listed in Table I. Given the magnitude of the discrepancy, it is important to ascertain whether this difference will persist in going from the one-dimer model to a more realistic representation of the surface. QMC gives energies in very good agreement with the MRCI results for Si_9H_{12} and, unlike traditional quantum chemistry methods, can be applied to larger models of the surface to study the convergence of the reaction energies with cluster size and access accurate estimates for the real surface.

In Table I, we list the PW91, B3LYP, and QMC adsorption, desorption, and reaction energies via the intradimer mechanism for the clusters with one, two, three, and four surface dimers. The QMC energies are consistently higher than the PW91 values for all clusters: The QMC adsorption, desorption, and reaction energies are above the PW91 values by about 0.3, 0.8, and 0.5 eV, respectively. Therefore, the corrections to the PW91 values due to the incorrect treatment of electronic correlation are indeed large, and, interestingly, they do not show a significant dependence on the size of the cluster. The QMC results for $Si_{27}H_{24}$ have a large statistical error bar but also demonstrate the smooth QMC convergence with system size. B3LYP represents a significant improvement upon PW91, giving energies which are much closer to our QMC results, and only lower by about 0.05, 0.2, and 0.15 eV for $Si_{21}H_{20}$. This is in accordance with earlier studies using the B3LYP functional for the Si-H system [11,19,25].

Interdimer H2 and H4 mechanisms.—In the H2 pathway, the hydrogen molecule dissociates over two clean neighboring Si dimers, yielding a cis configuration with

TABLE I. Adsorption (E_a^{ads}), desorption (E_a^{des}), and reaction (E_{rxn}) energies in eV for H_2/Si(001) via the intradimer H2* mechanism (see Fig. 1), calculated within PW91, B3LYP, and QMC. Zero-point energies (ZPE) are not included.

	PW91			B3LYP			QMC		
	E_a^{ads}	E_a^{des}	E_{rxn}	E_a^{ads}	E_a^{des}	E_{rxn}	E_a^{ads}	E_a^{des}	E_{rxn}
Si_9H_{12}	0.69	2.86	2.17	0.90	3.40	2.50	1.01 ± 0.06	3.65 ± 0.06	2.64 ± 0.06
$Si_{15}H_{16}$	0.56	2.65	2.09	0.71	3.20	2.49	0.98 ± 0.05	3.52 ± 0.07	2.54 ± 0.06
$Si_{21}H_{20}$	0.32	2.31	1.99	0.56	2.90	2.35	0.61 ± 0.05	3.11 ± 0.05	2.49 ± 0.05
$Si_{27}H_{24}$	0.37	2.35	1.98	0.57	2.91	2.33	0.49 ± 0.13	3.03 ± 0.13	2.54 ± 0.13

two hydrogens bound to two Si atoms at the same side of the dimers. For the H4 mechanism, the adsorption occurs on two neighboring Si dimers which are both already covered on the same side with hydrogens (see Fig. 1). The PW91, B3LYP, and QMC adsorption, desorption, and reaction energies for the H2 and H4 pathways are presented in Table II. All calculations were performed on the four-dimer cluster $Si_{27}H_{24}$ and the reaction occurs on the two central dimers. For both mechanisms, the results show the same trends as for the intradimer pathway: PW91 significantly underestimates reaction energies and the energy barriers, and B3LYP is much closer to the QMC results than PW91. For the H4 mechanism, PW91 and B3LYP predict no adsorption barrier. Within the statistical error, we find this to remain true also in the QMC calculation. To explore a possible QMC adsorption barrier, we computed the QMC energies for nine geometries along the path connecting the configuration of four hydrogens on two neighboring dimers with the configuration of two hydrogens in the cis configuration plus a desorbed hydrogen molecule. However, the cis configuration does *not* constitute the energetically lowest adsorption geometry of two hydrogens atoms and, thus, occurs only scarcely. The pairing energy, that is, the energy difference between the cis configuration and two hydrogens at the same Si dimer, is found to be 0.34, 0.42, and 0.54 ± 0.07 eV in PW91, B3LYP, and QMC, respectively [26].

Discussion and conclusions.—Using our accurate QMC energetics and the available experimental results, we can achieve a firm understanding of the physics of the interaction of hydrogen with the Si(001) surface. In order to analyze the various reaction pathways, we first need to extrapolate the QMC energies to the infinite-system limit and include the zero-point energy corrections (ΔZPE). We start from the PW91 infinite-system limit (the PW91 slab energy) and add a correction for the inaccurate treatment of electronic exchange and correlation estimated from the cluster calculation as $\Delta E_{\mathrm{corr}} = \mathrm{E}^{\mathrm{QMC}}_{\mathrm{cluster}} - \mathrm{E}^{\mathrm{PW91}}_{\mathrm{cluster}}$. This correction is computed using the $Si_{21}H_{20}$ cluster for H2* and $Si_{27}H_{24}$ for the H2 and H4 mechanisms. After including the ZPE contribution, the final QMC energy is $\mathrm{E}^{\mathrm{QMC}} = \mathrm{E}^{\mathrm{PW91}}_{\mathrm{slab}} + (\mathrm{E}^{\mathrm{QMC}}_{\mathrm{cluster}} - \mathrm{E}^{\mathrm{PW91}}_{\mathrm{cluster}}) + \Delta\mathrm{ZPE}$. In Table III, the extrapolated QMC energies are compared with the experimental results.

The barriers from PW91 slab calculations are significantly lower than the experimental results and, for desorption, the discrepancy is even amplified when the negative ZPE's are added. From our QMC results, we find that the corrections to PW91-GGA are very large: the reaction energy is underestimated by 0.5 eV and the adsorption and desorption energies by as much as 0.3 and 0.8 eV. Therefore, we conclude that PW91 is not a reliable tool to investigate systems with H-Si bonds.

The final QMC reaction energies are compatible with experiments, and the adsorption barriers are in much better agreement with the experimental results than the PW91 barriers. The larger adsorption barriers for the intradimer and the low-coverage H2 interdimer pathways can finally explain why the sticking coefficient on the clean Si(001) surface is so small at low temperatures. Moreover, the high reactivity for adsorption via the H4 mechanism is corroborated by the QMC results which are consistent with a barrierless pathway as recently proposed experimentally. Possibly, the dramatic increase in sticking probability with surface temperature is partly due to this pathway: if hydrogen is already present on the surface, an increase in surface temperature leads to an

TABLE II. Adsorption, desorption, and reaction energies in eV per molecule for H_2/Si(001) via the H2 and H4 mechanisms (see Fig. 1). The $Si_{27}H_{24}$ model cluster of the surface is used.

	E_a^{ads}	E_a^{des}	E_{rxn}
H2 mechanism			
PW91	0.26	2.24	1.99
B3LYP	0.54	2.87	2.33
QMC	0.59 ± 0.09	3.11 ± 0.09	2.52 ± 0.09
H4 mechanism			
PW91	0.00	2.46	2.13
B3LYP	0.00	2.91	2.50
QMC	0.19 ± 0.14	3.18 ± 0.12	2.61 ± 0.11

TABLE III. Extrapolated QMC adsorption, desorption, and reaction energies in eV for the H2*, H2, and H4 mechanisms (see text).

	E_a^{ads}	E_a^{des}	E_{rxn}
H2* mechanism			
E_{slab}^{PW91}	0.37	2.27	1.90
ΔZPE[a]	+ 0.09	−0.11	−0.20
ΔE_{corr}	$+0.29 \pm 0.05$	$+0.80 \pm 0.05$	$+0.50 \pm 0.05$
E_{QMC}	0.75 ± 0.05	2.96 ± 0.05	2.20 ± 0.05
Expt.	> 0.6[b]	2.5 ± 0.1[c]	1.9 ± 0.3[d]
H2 mechanism			
E_{slab}^{PW91}	0.20	2.15	1.95
ΔZPE[a]	+0.09	−0.11	−0.20
ΔE_{corr}	$+0.34 \pm 0.09$	$+0.87 \pm 0.09$	$+0.53 \pm 0.09$
E^{QMC}	0.63 ± 0.09	2.91 ± 0.09	2.28 ± 0.09
Expt.	> 0.6[b]	2.5 ± 0.1[c]	1.9 ± 0.3[d]
H4 mechanism			
E_{slab}^{PW91}	0.00	2.32	2.01
ΔZPE[a]	N/A	−0.20	−0.20
ΔE_{corr}	$+0.19 \pm 0.14$	$+0.72 \pm 0.12$	$+0.48 \pm 0.11$
E^{QMC}	0.19 ± 0.14	2.84 ± 0.12	2.29 ± 0.11
Expt.	0.00[b]	2.5 ± 0.1[c]	N/A

[a]Ref. [19] (identical ΔZPE assumed for all mechanisms).
[b]Ref. [7]. [c]Ref. [10]. [d]Ref. [27].

increased number of cis configurations, thus creating barrierless adsorption sites for sticking.

Concerning desorption, the picture is more complicated. Judging from the extrapolated QMC barriers, none of the studied mechanisms appears to be compatible with the desorption energy of 2.5 ± 0.1 eV observed in temperature-programmed desorption experiments [10]. However, such experiments could have been affected by a small concentration of surface imperfections. To exemplify this possibility, we looked at the adsorption/desorption of H_2 at the D_B step edge which is modeled as a $Si_{28}H_{28}$ cluster constructed from previous slab calculations [6]. Experimentally, a small adsorption barrier of 0.09 ± 0.01 eV is observed while PW91 predicts no adsorption barrier, so PW91 desorption and reaction energies are the same. Here, we compute only the B3LYP and QMC reaction energies for $Si_{28}H_{28}$, which are equal to 2.54 and 2.81 ± 0.07 eV, respectively. The extrapolated QMC value is 2.61 ± 0.07 eV, significantly lower than the other desorption barriers, and, hence, the presence of a small number of steps could dominate the desorption yield. Our calculations suggest that the hitherto accepted experimental value of the desorption barrier underestimates the barrier for an ideal Si(001) surface due to contributions from steps or defects.

In agreement with very recent experimental findings [28], the QMC calculations predict a slight preference for the H4 mechanism for experiments where contributions from surface imperfections are carefully avoided (e.g., by heating the surface only very locally). While the lack of an adsorption barrier along the H4 pathway can explain the low kinetic energy of the desorbing hydrogen molecules, one should also keep in mind the observed vibrational excitation in desorption [29], indicating that some molecules desorb on a pathway with an adsorption barrier. We conclude that several mechanisms contribute to desorption, whose relative importance depends sensitively on temperature, coverage, and surface perfection.

In this Letter, we presented accurate QMC calculations for various pathways of adsorption/desorption of H_2 from Si(001), using large cluster models of the surface. For all pathways, we find that PW91 significantly underestimates reaction energies and barriers when compared to QMC. Therefore, caution should generally be used when employing PW91 or other GGAs in the study of H-Si bonded systems. In view of the wide usage of DFT calculations as a tool in materials science, our findings could have important consequences for other fields, in particular, for studies of heterogeneous catalysis and hydrogen-bonded systems. The QMC adsorption barriers are in close agreement with experimental values and support recent experimental findings. Finally, the results for desorption call for further experimental studies of the activation energy and its dependence on coverage and surface perfection.

[1] M. Dürr, M. B. Raschke, and U. Höfer, J. Chem. Phys. **111**, 10 411 (1999).
[2] K. W. Kolasinski *et al.*, Phys. Rev. Lett. **72**, 1356 (1994).
[3] E. Pehlke and M. Scheffler, Phys. Rev. Lett. **74**, 952 (1995); P. Kratzer, B. Hammer, and J. K. Nørskov, Phys. Rev. B **51**, 13 432 (1996); A. Gross, M. Bockstedte, and M. Scheffler, Phys. Rev. Lett. **79**, 701 (1997).
[4] F. M. Zimmermann and X. Pan, Phys. Rev. Lett. **85**, 618 (2000).
[5] A. Biedermann *et al.*, Phys. Rev. Lett. **83**, 1810 (2001).
[6] P. Kratzer *et al.*, Phys. Rev. Lett. **81**, 5596 (1998).
[7] M. Dürr *et al.*, Phys. Rev. Lett. **86**, 123 (2001).
[8] M. Dürr *et al.*, Phys. Rev. Lett. **88**, 046104 (2002).
[9] E. Pehlke, Phys. Rev. B **62**, 12 932 (2000).
[10] U. Höfer, L. Li, and T. F. Heinz, Phys. Rev. B **45**, R9485 (1992).
[11] P. Nachtigall *et al.*, J. Chem. Phys. **104**, 148 (1996).
[12] M. R. Radeke and E. A. Carter, Phys. Rev. B **54**, 11 803 (1996).
[13] Z. Jing and J. L. Whitten, J. Chem. Phys. **98**, 7466 (1993); **102**, 3867 (1995).
[14] W. M. C. Foulkes *et al.*, Rev. Mod. Phys. **73**, 33 (2001).
[15] S. B. Healy *et al.*, Phys. Rev. Lett. **87**, 016105 (2001).
[16] E. Penev, P. Kratzer, and M. Scheffler, J. Chem. Phys. **110**, 3986 (1999); in improvement over this work, transition states were reoptimized, and energies calculated for a plane-wave basis set with a cutoff up to 40 Ry.
[17] J. P. Perdew, in *Electronic Structure of Solids '91*, edited by P. Ziesche and H. Eschrig (Akademie Verlag, Berlin, 1991), pp. 11–20.
[18] A. D. Becke, J. Chem. Phys. **98**, 5648 (1993); C. Lee, W. Yang, and R. G. Parr, Phys. Rev. B **37**, 785 (1988). Fully self-consistent B3LYP calculations are performed for the clusters. B3LYP requires the calculation of exchange integrals, and this makes this functional computationally very expensive; hence, we have not used B3LYP in the context of plane-wave calculations for slabs.
[19] J. A. Steckel *et al.*, J. Phys. Chem. B **105**, 4031 (2001); in Table IV, the angles for the geometries optimized in B3LYP are 3.3, 12.6, and 13.1° for reactant, TS, and product, respectively.
[20] P. J. Reynolds *et al.*, J. Chem. Phys. **77**, 5593 (1982); L. Mitas, E. L. Shirley, and D. M. Ceperley, *ibid.* **95**, 3467 (1991); C. J. Umrigar, M. P. Nightingale, and K. J. Runge, *ibid.* **99**, 2865 (1993).
[21] C. Filippi and C. J. Umrigar, J. Chem. Phys. **105**, 213 (1996).
[22] The Gaussian basis sets are $(10s10p1d)/[3s3p1d]$ for silicon and $(10s1p)/[3s1p]$ for hydrogen and are optimized at the HF level for the Si_9H_{12} cluster.
[23] M. W. Schmidt *et al.*, J. Comput. Chem. **14**, 1347 (1993).
[24] C. J. Umrigar, K. G. Wilson, and J. W. Wilkins, Phys. Rev. Lett. **60**, 1719 (1988).
[25] Y. Okamoto, J. Phys. Chem. B **106**, 570 (2002).
[26] The PW91 slab value for the pairing energy is 0.31 eV.
[27] M. B. Raschke and U. Höfer, Phys. Rev. B **63**, R201303 (2001).
[28] M. Dürr *et al.*, Science **296**, 1838 (2002).
[29] K. W. Kolasinski, S. F. Shane, and R. N. Zare, J. Chem. Phys. **96**, 3995 (1992).